Control Application in Renewable Generation

John Ringwood, Maynooth University, Center for Ocean Energy Research, Maynooth, Co. Kildare, Ireland

Abstract

While many control problems fall into the general category of regulation or setpoint following, the control of renewable energy systems has a wider variety of objectives, including energy conversion maximization or minimization of the cost of the converted energy. Given the intermittent and potentially unpredictable nature of many renewable energy sources, there may also be objectives related to matching supply with demand. This chapter focuses primarily on intermittent renewable energy sources, such as wind, wave, tidal, solar, while some consideration is also given to salinity gradient, and ocean thermal. This chapter discusses resource and system modeling, and outline solutions to typical renewable energy control problems.

Key Points

- Provision of an overview of renewable energy systems and their characteristics.
- Examination of a selection of renewable energy systems and their control needs.
- Selection of appropriate control methods from the body of control tools available.
- Presentation of an application study, which shows detailed application of control to a renewable energy system.

Introduction

In order to establish the scope for this chapter, some definition of renewable energy systems is required. In addition, within the space limitations of this chapter, it would be impossible to deal with every renewable energy technology, so some `useful' subset will be examined, to allow some level of detail to be covered. In particular, hydro and biomass are excluded from the current analysis, since they are relatively mature technologies, are effectively dispatchable, and biomass/biofuel production falls under the category of process control. In general, renewable energy resources are deemed to be resources that are replenished at a higher rate than they are consumed. Clearly, fossil fuels do not fall into this category, since they have taken millenia to form, and are therefore seen as a finite resource. In addition, with the climate action imperative, there is a necessary focus on energy conversion modes which don't release greenhouse gasses.

In a bid for zero-carbon energy provision, a wide variety of renewable energy forms are being considered (Qazi *et al.*, 2019). Given the relatively deep, and increasing, penetration of onshore wind and solar, there is a need to complement these intermittent renewable sources with a broader set of renewable sources so that their combination can provide something close to dispatchable energy (Jurasz *et al.*, 2020; Sinsel *et al.*, 2020). A potential solution to match renewable supply to demand exists in the availability of suitable energy storage; however, the current cost of adequate storage is somewhat excessive. Nevertheless, the control of the entire grid system with a high penetration of renewables, in matching supply to demand, utilizing storage, and preserving grid stability, while ensuring economic operation, is an important area of control, but beyond the scope of this chapter. The interested reader is referred to Alam *et al.* (2020); Ourahou *et al.* (2020); Tan *et al.* (2021).

This chapter will focus primarily on natural environmental resources, such as wind, solar, etc, since these, in general, provide the greatest control challenges, due to their less predictable nature. This is in contrast to, say, biomass, which is a form of synthetic fuel manufacture. While there is strategic value in having an optimal complement of renewables to provide resilient supply, the current predominant driver is currently cost, typically articulated as the levalised cost of energy (LCoE):

$$LCoE = (\mathrm{CapEx} + \mathrm{OpEx})/(\mathrm{Power\ \ production}), \tag{1}$$

where CapEx denotes capital expenditure (in \$,€), OpEx (in \$,€) denotes operational expenditure, and power production is measured in W. In general, control has a primary effect on power production, though it may also affect OpEx, due to the possible detrimental effect of aggressive control action on the maintenance requirements of a device. In open energy markets, the real-time cost of energy determines what resources will be scheduled at any given point in time, but LCoE is the main driver for *investment* in renewable technology.

Table 1 shows a range of renewable energy sources and their current LCoE values, together with some indicators regarding intermittency and predictability. In general, nascent renewables, such as ocean renewable energy (ORE, which excludes offshore wind) are significantly higher in cost, and cost uncertainty. Yet, ORE represents a considerable untapped resource and could, in many cases, complement more established renewables, such as wind, (Fusco *et al.*, 2010) given their different characteristics.

This chapter examines the often crucial role that control technology has in maximizing the benefit of capital investments in renewable energy systems. The remainder of the chapter is organized as follows: Section "Brief Overview of Renewable Energy Systems" details a variety of renewable energy systems and examines the potential role for control in each. Section "Control Objectives" examines the range of possible control objectives associated with the range of renewable energy technologies, and discusses the challenges of directly addressing each. Section "Control Solution Domain" explores the control solution domain, highlighting various promising control solution candidates for renewable energy systems. A typical renewable energy application case study is documented in Section "Application Study", while conclusions are drawn in Section "Conclusions".

Table 1 Renewable resource global levels and characteristics

Resource	*Constant/ Intermit.*	*Pred/ Unpred.*	*Level TWh.a^{-1}*	*LCoE €(MWh)$^{-1}$*
Tidal energy	Intermit.	Pred.	26,000	97
Wave energy	Intermit.	Unpred.	32,000	228
Salinity grad.	Constant[a]	Pred.	1650[b]	97–264
OTEC	Constant[a]	Pred.	44,000	26–194
Offshore wind	Intermit.	Unpred.	340,000	98
Onshore wind	Intermit.	Unpred.	872,000	30
Solar PV	Intermit.	Pred.	$15{,}768 \times 10^4$	41

Note. [a]denotes constant, but with seasonal variation.
[b]while denotes technical, rather than theoretical, resource.

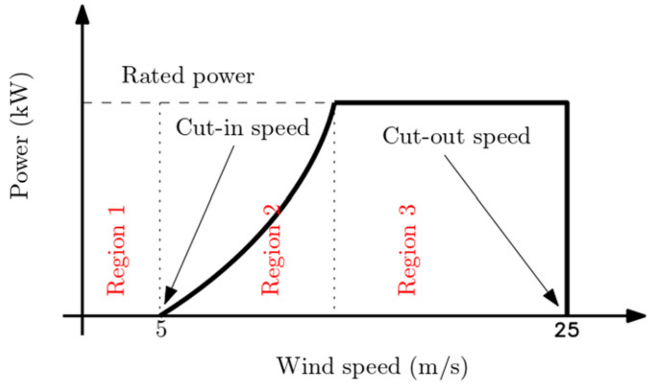

Fig. 1 Typical wind turbine power curve. In Region 2 the objective is to maximize converted power while, in Region 3, the goal is to remain withing the system rated power specification.

Brief Overview of Renewable Energy Systems

Wind Energy

The wind energy field can be broadly divided into onshore and offshore domains, while offshore wind can be further subdivided into fixed offshore and floating offshore. Unsurprisingly, the control problems associated with floating offshore turbines are more challenging than those for fixed (onshore or offshore) devices.

Onshore wind

Onshore wind is now a relatively mature renewable energy source, with significant developments over the past 5 decades (Hau and Renouard, 2006). It is now not uncommon to see horizontal-axis wind turbines of up to 15 MW, with further increases in capacity expected. The bulk of commercial wind turbines are horizontal-axis turbines, with vertical axis turbines being more common in niche applications (Hand *et al.*, 2021).

In general, the wind turbine control problem, consisting of torque and pitch control, is well understood, (Johnson *et al.*, 2006) but it is worth recalling that, in torque control mode (Region 2 in **Fig. 1**), the control objective is to maximize the power coefficient (see **Fig. 2**), by choosing optimal values of tip-speed ratio λ^o and blade pitch β^o.

$$\lambda = \frac{\omega^t R_t}{v_w} \tag{2}$$

where ω_t is the rotational speed (rads/sec) of the turbine, R_t is the rotor radius (m), and v_w is the wind velocity (m/s) and, assuming knowledge of v_w, the optimal turbine speed setpoint ω_t^o is determined, which is achieved via a speed regulation control loop, with turbine torque as the manipulated variable. This control strategy follows the general form of **Fig. 17** which is also typical of other MRE applications, such as tidal (see Section "Tidal Energy") and wave (Section "Wave Energy") energy.

Other key aspects of wind turbines include the ability to spill power, using blade pitch control, when the turbine reaches rated power, and the need for measurement of the incident wind speed to determine ω_t^o. Wind speed measurements, required as an input to the optimal determination of turbine rotational speed, are provided by individual annemometers on each turbine, though the forced placement of the annemometer in the wind shadow of the rotor complicates accurate wind speed measurement. However, commercial wind farms usually also have a separate (remote) pylon dedicated to wind speed measurement. The potential need for wind speed prediction is covered in Section "Control Solution Domain".

As wind turbines become larger, the issue of wind speed variations between the rotor bottom and top become significant. In order to avoid off-axial loads, which can be damaging for the machinery and bearings in the nacelle, individual blade pitch control can be employed, providing an interesting multivariable control problem (Selvam *et al.*, 2009). An associated issue relates to the need to estimate the loads on each turbine blade (Jelavić *et al.*, 2010).

Considering a slightly broader scale, individual pitch control can also be used for turbine wake steering to optimize overall wind *farm* energy conversion performance (Frederik *et al.*, 2020). However, in general, the interaction between turbines in a wind farm is destructive, which is characteristic of many renewable energy `farms', with an exception in wave energy (Section "Wave Energy").

One final issue is the value of short-term wind speed prediction, which can compensate for delays in actuation and/or the use of predictive techniques (covered in more detail in Section "Control Solution Domain"). For example, (Narayana *et al.*, 2009) articulate, and quantify, the benefits of advance wind speed information within a predictive control structure.

Offshore wind

In general, offshore wind turbines follow onshore designs, with the principal differences relating to the size of turbines used (offshore turbines are generally larger) and the progression to floating structures, as shown in **Fig. 3**, as water depth increases.

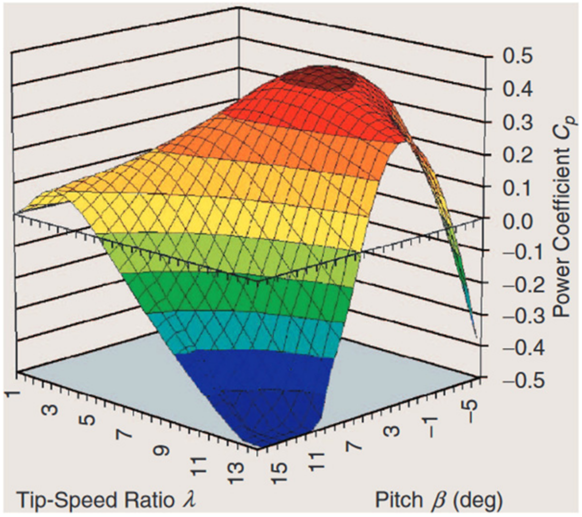

Fig. 2 Typical wind turbine power coefficient surface. From (Johnson *et al.*, 2006).

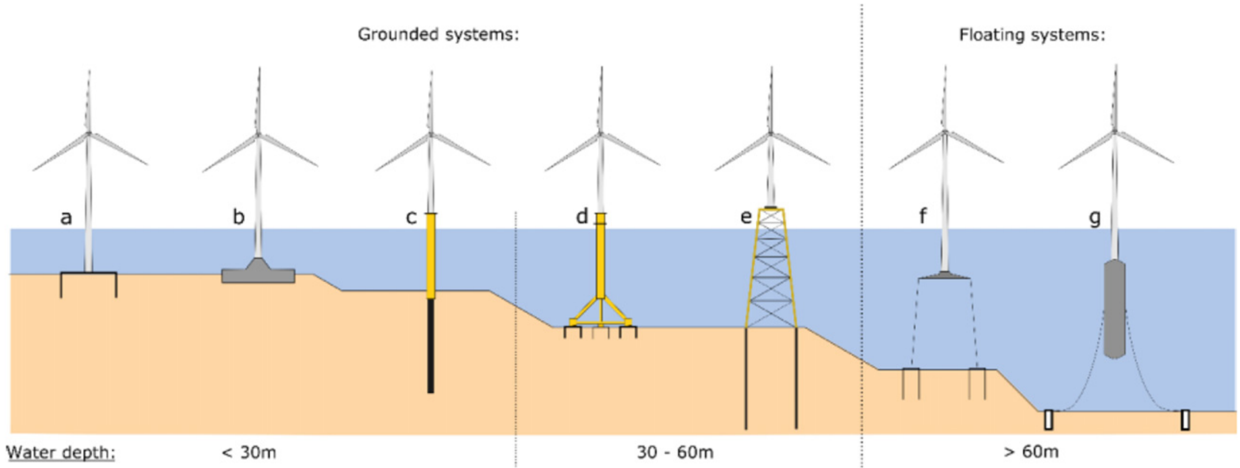

Fig. 3 Offshore wind turbine foundation/mooring options, in the move from shallow to deeper water. From (Bhattacharya *et al.*, 2018).

In particular, note that options f (tension leg) and g (loose mooring) involve floating platforms, where hydrodynamics need to be considered in the overall system model, with wave action causing potentially undesirable pitching, rolling, or surging motion on the turbine pylon.

However, other aspects, specific to the offshore scenario, are noteworthy, particularly for floating platforms (items f and g in **Fig. 3**, typically pitch motion induced by wave action co-incident with wind direction, and can produce:

- Cycling of the turbine pitch control system (which may lead to premature deterioration in pitch actuator mechanisms),
- Cyclical loading on the turbine tower, and/or
- Adverse cyclical loading on the mooring system.

A number of these issues, relating to control strategies, are considered in Skaare *et al.* (2007) while various strategies to counteract platform pitching have been proposed, including use of the pitch actuators themselves (Fontanella and Belloli, 2021) while an innovative wind/wave system was proposed by Fenu *et al.* (2020) which provides simultaneous platform stabilization and wave power capture through the use of a gyroscopic power take-off (PTO) system, while oscillating water column wave energy converters were incorporated into the pillars of a semi-sub floating offshore wind turbine (FOWT) in Sarmiento *et al.* (2019).

Tidal Energy

Despite being driven by the same gravitational mechanisms, tidal stream (exploiting tidal ocean currents) and tidal barrage (exploiting slow variations in mean sea level) technology differ significantly in terms of the devices employed, and the associated

Fig. 4 The Annapolis tidal barrage, generating on the ebb tide. From (Khare *et al.*, 2018).

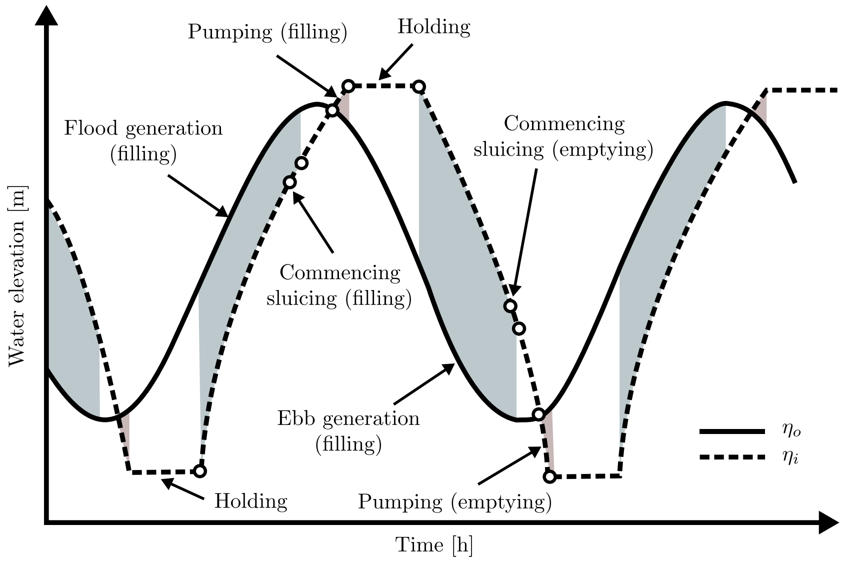

Fig. 5 Modes of operation of a tidal barrage, generating on both flood and ebb (based on (Angeloudis *et al.*, 2018)).

control problems. As the tidal `wave' proceeds around the earth, with a typical open ocean amplitude of $\sim$ 0.6 m, at restricted channel widths the flooding tide induces a tidal flow (due to water level difference) of up to 5 m/s, while certain estuaries which have a length L relative to the tidal wavelength λ_t of:

$$L_e = \frac{k\lambda_t}{4}, \quad k \quad \text{an odd integer} \tag{3}$$

create a resonance effect, significantly amplifying the 0.6 m open-ocean range. A prominent example includes the Severn estuary in the UK, with a (spring) tidal range of over 12 m. The tidal period is $\sim$ 12.5 h, related to the mean lunar day, with longer cycles due to relative positioning of the Sun, Moon and Earth.

Tidal barrages

The first commercial tidal barrage became operational in 1966 at the La Rance estuary in France, rated at 240 MW, while the Annapolis barrage (see Fig. 4), located at the Bay of Fundy in Canada, opened in 1984, with a rating of 20 MW.

With essentially monochromatic harmonic forcing, the objective is to maximize the value of the potential energy due to the water level difference on either side of the barrage, forcing the water through turbine ducts in the barrage to generate electricity. However, normally, the rate of filling/emptying through the turbine ducts is not sufficient to take full advantage of the tidal range variations and additional techniques of sluicing, pumping and holding are employed, as shown in Fig. 5. Note that generation may take place on flood only, ebb only, or both flood and ebb.

From Fig. 5, the optimal duration of each operational mode needs to be determined, noting that sluicing (though separate sluice gates) and generation (through the turbine ducts) can take place simultaneously. This has been set up as an optimal control problem by a number of researchers, with (Ryrie, 1995) and (Shen and Nyman, 2021) proposing schemes based on Bellman's

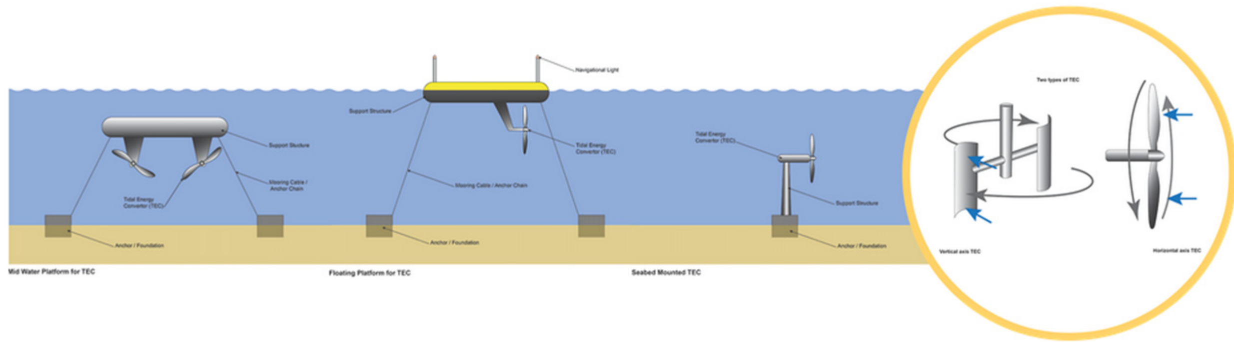

Fig. 6 Options for harnessing tidal stream. From (Morlais, 2022).

dynamic programming, and nonlinear model predictive control, respectively. The manipulated variables used in these studies are the flow into (or out of) the basin $q(t)$, and the number of turbines n (giving a discrete-level control), respectively. However, neither study captures the full set of operational modes in **Fig. 5**, including sluicing.

More recently, an optimal control approach, initially born within the wave energy domain, was applied to tidal barrages (Ringwood and Faedo, 2022). The technique uses a moment-based system description (according with the harmonic nature of the system variables and forcing function) and integrates generation, sluicing, and pumping seamlessly within the formulation.

Tidal stream

Tidal stream energy relies on technology not dissimilar to that for wind, with the important difference that water density is approximately 1000 times that of air (1025 kg/m^3 for sea water, 1.225 kg/m^3 for air). This leads to significantly small turbines for similar power ratings, with both vertical and horizontal axis devices employed, as for the wind case. Tidal turbines can be situated near the sea surface, suspended from floating platforms, bottom mounted, or suspended at an intermediate depth, as shown in **Fig. 6**, which also illustrates vertical and horizontal axis turbines.

In general surface or floating devices have a higher initial capital cost, but have the advantage of ease of access for maintenance, deployment, and recovery. Bottom mounted devices also have the disadvantage of being subject to bottom scour and tap a reduced tidal flowrate, due to the flow velocity shear effect close to the seabed.

In terms of control systems, tidal turbines have similar needs as wind turbines (see Section "Wind Energy"), with the exception that the range of tidal flow is known exactly so that the device can be highly optimized, and no cut-out point is needed. Some drawbacks, compared to wind turbines, include the need to operate in bi-directional mode, with no active yaw usually available. This is relatively easily achieved with floating devices, where the device naturally `weather-vanes' into the oncoming tide (via a swing mooring), while bottom-mounted turbines must work in both directions. Variable pitch turbines are not as ubiquitous as in the case of wind, given the harsher environment and susceptibility to water ingress. In many cases, the lost power is compensated by the reduced CapEx and OpEx, while the fixed tidal velocity operating range also reduces the imperative for pitch control.

Currently (Walker and Thies, 2021) no tidal stream installations can be truly described as commercial, with typically single device deployment, or small multiples ($\sim$3), with overall generating capacity typically less than 1 MW. However, Orbital Marine (Orbital Marine Power, 2024) have been testing a floating 2 MW machine (the O2) since 2021.

Wave Energy

Wave energy is at a similar stage of development as tidal stream, in that full-scale grid connected prototypes have been deployed, but no commercial wave energy farms are, as yet, operational, despite rudimentary wave energy devices proposed as early as the 19th century. However, one distinctive feature of wave energy technology is the great diversity in operating principles and resulting device types (see **Fig. 7**), leading to a lack of technology convergence, with over 200 prototypes reported (Koca *et al.*, 2013). Wave devices can harness either the potential or kinetic energy arising from wave motion, with a variety of PTO mechanisms used to convert the wave energy to a useful form. The pressurized seawater produced by certain PTO mechanisms can also be used to drive reverse osmosis systems (Bacelli *et al.*, 2009) as well as conversion to electricity.

In particular, the reciprocating energy flux of wave motion presents a challenge, with the need for rectification at some stage (hydrodynamic, mechanical, pneumatic, electrical) to produce unidirectional power flow. In addition, the high force/low velocity characteristics generally do not suit electrical machines, with a general difficulty in implementing any form of `gearing' to alter the force/velocity balance.

A further difficulty with wave energy is that ocean waves are described by a spectrum, which itself is sea-sate dependent, for example as shown in **Fig. 8**. For many devices (e.g point absorbers) which resonate, the challenge is to adapt the device resonant

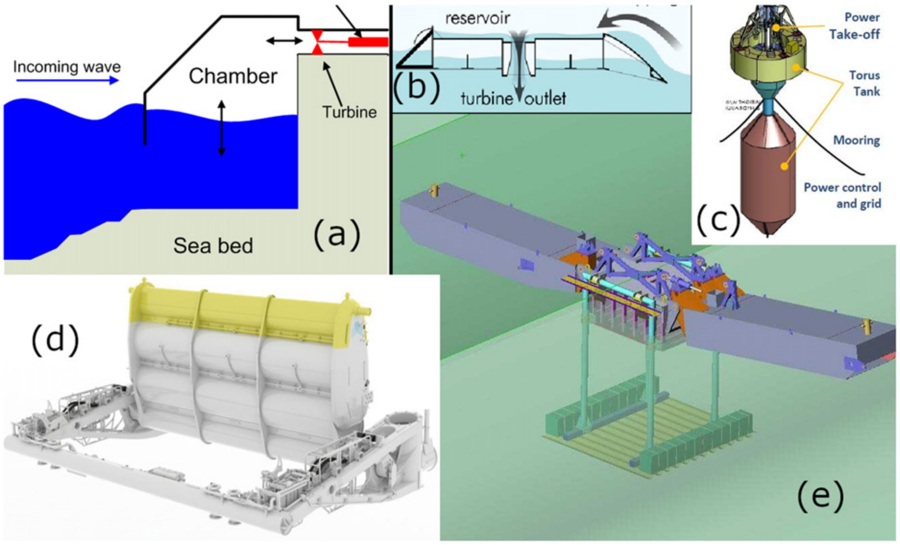

Fig. 7 Some WEC operating principles: (a) Oscillating water column, (b) overtopping device, (c) self-referenced point absorber, (d) Oscillating wave-surge converter, and (e) hinge-barge device.

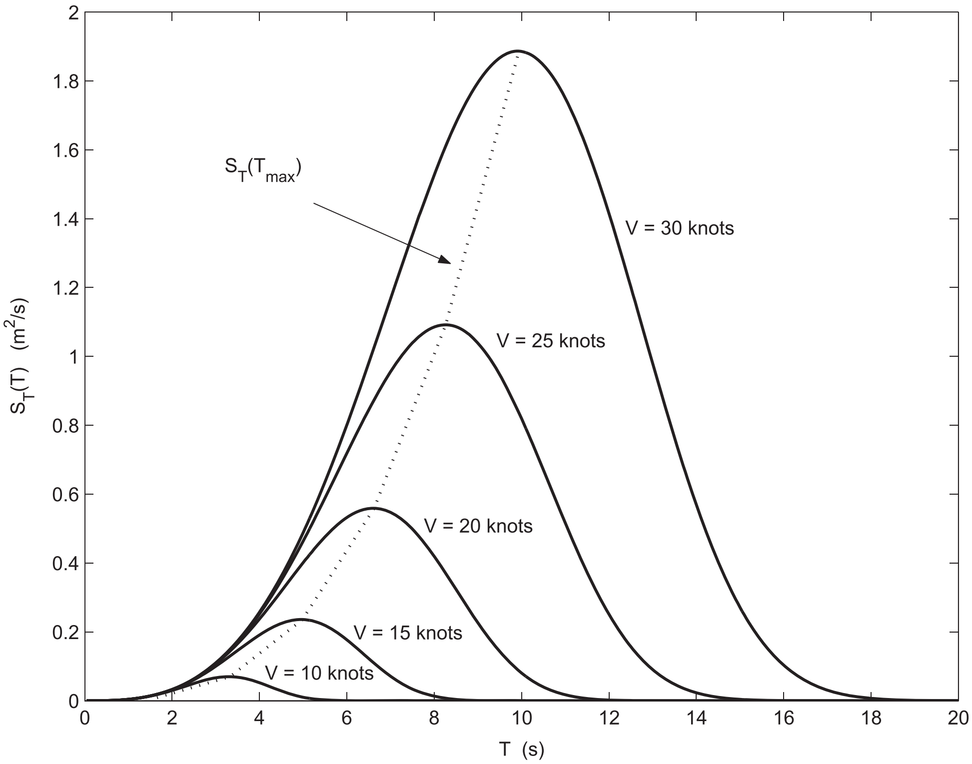

Fig. 8 Pierson-Moskowitz fully-developed wave spectrum resulting from various wind velocities.

frequency on a wave-by-wave and sea-state basis. For many WECs, the control problem then presents itself with the structure of Fig. 17, where the setpoint determination corresponds to the optimal velocity profile, with the lower loop then following the desired velocity profile. If the system can be described by a linear model, the setpoint determination problem reduces to one of impedance matching (Ringwood *et al.*, 2014). However, since optimizing controllers for wave energy devices can *exaggerate* the motion of WECs through the use of reactive power, the linearizing assumption (small motion about equilibrium) is often challenged (Windt *et al.*, 2021). Recently, MPC-like WEC control techniques, using adapted performance functions based on

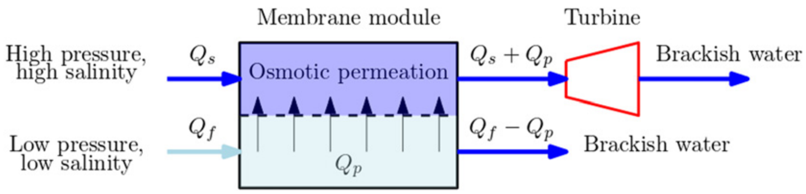

Fig. 9 Pressure retarded osmosis (PRO).

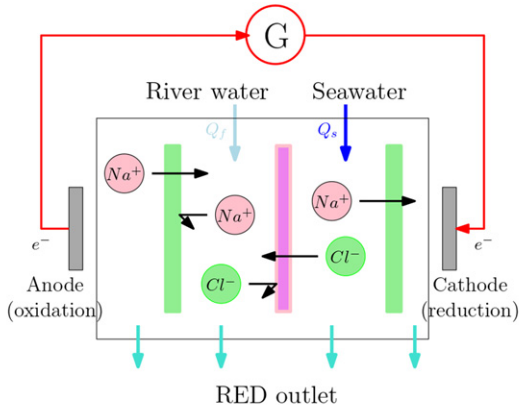

Fig. 10 Reverse electrodialysis (RED).

energy maximization, have been employed, which (crucially) also manage physical device constraints on force and displacement (Ringwood *et al.*, 2014).

Salinity Gradient

Salinity gradients exist between freshwater and seawater and two broad classes of practical methods exist to convert this gradient into useful energy, namely:

- Pressure retarded osmosis (PRO), (Gonzales *et al.*, 2021) and
- Reverse electrodialysis (RED) (Tufa *et al.*, 2018).

Other methods, though less practical, based on vapor pressure differences, methods using nanotubes, and capacitive methods, also exist.

Pressure retarded osmosis

In PRO, the osmotic effect of the salinity gradient is harnessed to create a pressure increase, as shown in **Fig. 9**, with water transport across the membrane following the direction of *negative* salinity gradient. The fluid pressure increase, in turn, is used to drive a turbine which can be connected to an electrical generator. Statkraft (Norway) opened the world's first PRO plant in 2009, with a rating of 10 kW, and design of a 2 MW power plant was finalized and a permit obtained in 2013. However, at the end of 2013, Statkraft decided to discontinue their investment in osmotic power, citing a lack of long-term financial support mechanisms (Kempener and Neumann, 2014). More recently, hybrid systems, combining a number of other technologies and objectives with PRO, such as desalination and wastewater treatment, have shown promise, lowering the effective energy cost and increasing overall efficiency (Gonzales *et al.*, 2021).

From a control systems perspective, there are several aspects which merit consideration. While maximum turbine (and hence generator) power might be an obvious control objective, a broader consideration of LCoE as defined in (1) is necessary. In particular, OpEx can be considerable, due to the parasitic energy requirements on saltwater Q_s and freshwater Q_f pumping, pressurization, and pre-treatment, and careful management of the membrane, in terms of both fouling minimization, and avoidance of damaging differential pressure excesses, is required. Also, care must be taken with the discharge of high salinity concentrations of byproducts (i.e., brine) to mitigate environmental impact of direct ocean discharge. For hybrid systems, the control objectives, and range of manipulated variables, may be even broader, leading to a rich constrained multivariable control problem with multiple objectives. To the best of this author's knowledge, few attempts have been made to present this set of challenges as a formal control problem, and perhaps control may be an important ingredient that may tip the commercial balance for PRO and its hybridized versions.

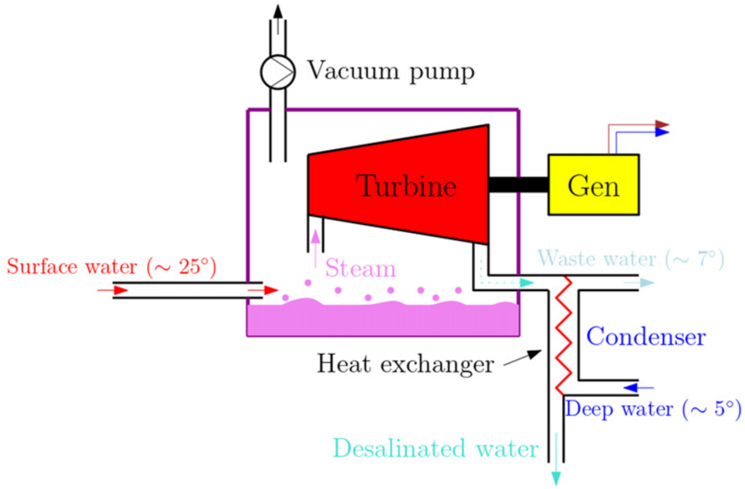

Fig. 11 Open-cycle OTEC system.

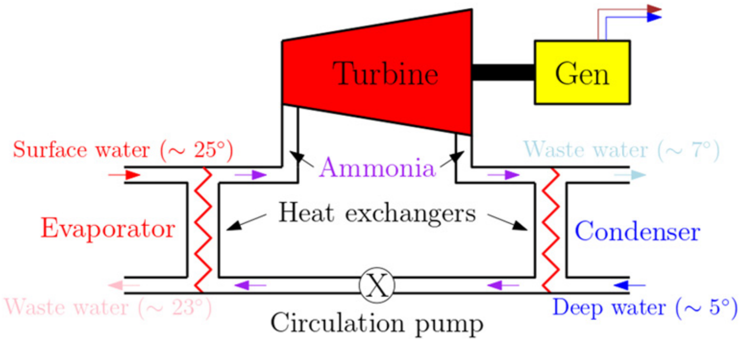

Fig. 12 Closed-cycle OTEC system.

Reverse electrodialysis

In RED, membranes are also employed, but their function (and the materials used) is significantly different from PRO, with RED membranes facilitating the selective transport of salt ions in different directions, as shown in **Fig. 10**. Two substances, with different salt concentrations, pass through a stack of alternating cathode and anode exchanging permselective membranes. The compartments between the membranes are alternately filled with sea water and fresh (or low-salt) water. The salinity gradient difference is the driving force for the transport of ions that results in an electric potential that is then *directly* converted to electricity. The total electricity output is determined by the sum of the potential difference over all the membranes, with various series/parallel configurations possible.

The first RED process was described by Pattle (1954) though the technology has still to become commercial. A 50 kW RED pilot plant was built in 2013 at the interface between the North Sea and the Ijsselmeer at Breezanddij, Netherlands, due to be upscaled to 1 MW by 2020, (Tufa *et al.*, 2018) but no further progress on this has been reported. As with PRO, various hybrid schemes can improve the efficiency and economy of RED processes, including wastewater treatment and water desalination, and RED has also been proposed as a storage device, via hydrogen production (Tufa *et al.*, 2018).

A parametric evaluation of feed concentration, feed flow rate, and temperature, to identify the optimal working conditions of an industrial-scale RED unit, was carried out by, (Tristán *et al.*, 2020) which could be considered an initial analysis into the optimal control of RED systems.

OTEC

Ocean thermal energy conversion (OTEC) is, in essence, a heat engine, exploiting the relatively shallow thermal gradient between surface seawater, at a temp. of around 25°, and water from depth (typically 1 km), at around 5°. Both open- and closed-cycle (**Figs. 11** and **12**, respectively) configurations are possible. Open cycle has the advantage of producing desalinated water as a by-product, while also not requiring a third medium (e.g. ammonia) with a low boiling point. Both configurations consume a significant amount of parasitic energy, estimated at 30% with pumping required for both surface and deep water, as well as a vacuum pump (open cycle) and a refrigerant loop (closed cycle).

OTEC plants can be sited onshore (fixed) or offshore (floating), at locations which have a relatively high surface water temperature and considerable water depth. A number of pilot-scale installations are in operation, (Herrera *et al.*, 2021) including the 100 kW plant on Kume Island, Japan (2013), and the closed-loop 105 kW OTEC plant in Kona, Hawaii. However, commercial-scale OTEC plants are under development in Martinique (10.7 MW) and Deigo Garcia Island (13 MW).

Various studies have examined the technological requirements of OTEC (e.g., (Cohen, 2009; Langer *et al.*, 2020)), though none have focussed on control as an enabling technology. The single control-oriented OTEC study available (He *et al.*, 2018) is focussed on control of the motion of a floating OTEC system, rather than the process itself.

Solar Energy

Solar energy divides broadly into harnessing energy through solar heating, and direct conversion into electricity though photovoltaic (PV) cells. Both present interesting, and diverse, control problems. One control problem, common to both solar thermodynamic and PV, is the constant re-orientation of mirrors or solar cells to ensure maximum reflection/absorption of the sun's rays. This is a relatively standard tracking control problem, and will not be further dealt with here. The interested reader is referred to the review by Fuentes-Morales *et al.* (2020) and Awasthi *et al.* (2020) for further information. One of the main challenges in the optimal control of solar systems is maximizing power capture as the sun arcs through the sky, with potential short-term variation in cloud cover, both leading to variation in the amount of raw solar energy available. An overview of the control of both types of solar energy systems is available in Camacho and Berenguel (2012).

Solar heating

Solar heating ranges from the use of domestic solar panels, which can essentially be considered as heat exchangers, to grid-scale thermodynamic solar plants. These grid-scale systems utilize an array of mirrors to concentrate the sun's rays onto a `receiver' containing a heat-carrying liquid. The concentrated heat transforms the liquid into steam which is, in turn, used to drive a turbine connected to an electrical generator. This is not unlike the heat exchanger system shown in **Fig. 12**, though the temperatures in the solar case are significantly higher, with no vacuum needed to flash the liquid into steam. A detailed analysis of thermodynamic solar system control is given by, (Camacho and Berenguel, 2012) with **Fig. 13** showing a commercial solar heating installation.

Solar PV

Solar photovoltaics (PV) are now a popular renewable energy source, with installed global capacity set to reach 2 TW in 2024, (Allouhi *et al.*, 2022; International Energy Agency , 2023) including both grid-scale and distributed micro-generation. A wide variety of

Fig. 13 20 MW thermodynamic solar plant near Seville (Camacho and Berenguel, 2012).

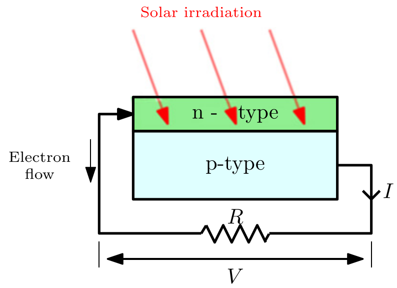

Fig. 14 Basic components of a solar PV cell.

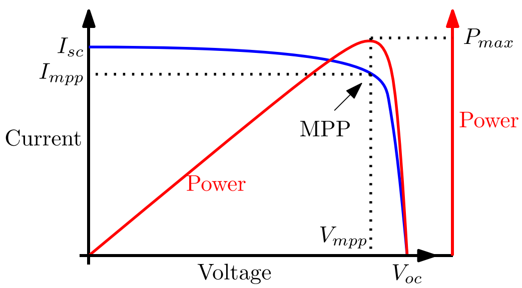

Fig. 15 Solar PV cell $I - V$ characteristic. MPP indicates the maximum power point where the $I - V$ product is a maximum.

optimization and control methods have been applied to solar PV systems, many focussing on system design, with purely economic performance functions, (Al-Shahri *et al.*, 2021) while control systems are employed at the technical operational level to maximize conversion efficiency. A basic illustration of a solar PV cell is shown in **Fig. 14**. The essential control objective is to maximize power transferred to the load (IV) by manipulation of the effective load resistance R. **Fig. 15** shows the typical $I - V$ curve for a solar cell. The main control objective is to continuously adjust the effective load resistance so that the $I - V$ product is a maximum.

In addition to PV panel orientation, and control of the load, one other control-related aspect is significant, focussed on the need to maintain the PV panel at an efficient working temperature (Sharaf *et al.*, 2022). For example, active water cooling can lead to a 20% temperature reduction, with a consequent 9% efficiency enhancement. However, active cooling also represents a parasitic energy requirement, which may offset some/all of the efficiency gains, depending on the system. The sensitivity of PV efficiency to surface temperature variations is indicated in **Fig. 16**. Control aspects, relating to PV cooling are not covered here, since cooling control systems are well documented in the literature; the interested reader is referred to (Sharaf *et al.*, 2022).

Control Systems for Renewable Energy

Control Objectives

A range of control objectives can be considered in relation to renewable energy systems. One important consideration is that, while the raw energy itself is free, the cost of converting it is not. This in sharp contrast to, for example, fossil fuels, where energy conversion efficiency is important. Efficiency, in the renewable energy domain, is a somewhat misleading technical objective, though beloved of engineers! Ultimately, from (1), it should be clear that, even if efficiency is low (i.e. power production is low), this is not important so long as CapEx and OpEx are correspondingly lower. It may be that a cheap devise, operated well, may be optimal from an LCoE perspective.

While maximization of energy capture might seem paramount, for a given CapEx and OpEx, this assumes that control actions to maximize energy capture have no deleterious effects on CapEx or OpEx in (1). While this may be true in some systems, excessive cycling of actuators (e.g., in wind turbine blade pitch control), or aggressive control actions (e.g., in wave energy systems), may significantly impact OpEx, in particular.

While LCoE in (1) is a reasonable economic objective, it places no importance on the time at which energy is produced, which is a critical aspect of renewable energy systems. In the absence of additional storage, producing energy on demand might seem to be an unreasonable objective for intermittent, and often unpredictable, renewable energy resources. However, the are some possibilities:

- Tidal barrage systems contain an amount of storage, but the storage capacity is dependent on the state of the external ocean water level, which is constantly changing, and

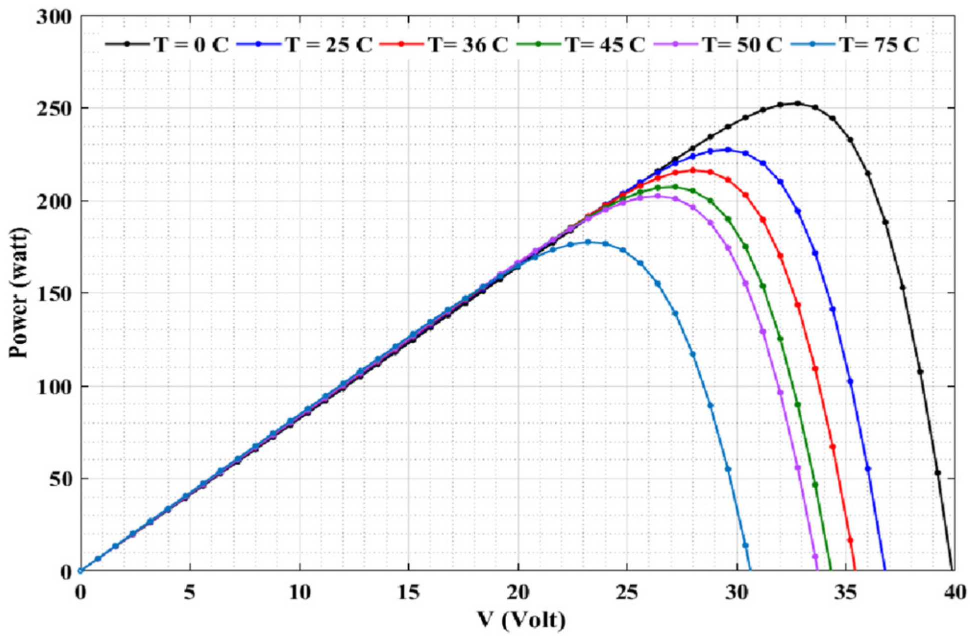

Fig. 16 Temperature sensitivity of solar PV (Ibrahim *et al.*, 2021).

- The wear on the system in operational mode may not be worth the marginal price of electricity.

However, the possibilities above represent a minority of situations and, in addition, the connection between OpEx in (1) and control actions is difficult to articulate. Considering these issues, the control objective for renewable energy systems usually reduces to maximization of energy converted, since there is a clear and deterministic connection between control actions and energy converted. From a broad perspective, it seems reasonable that the maximum utility should be made of a renewable energy asset, for a given capital outlay. That said, some attention is now being paid to broader control objectives (e.g. goal-oriented control), (Chen, 2024) while economic MPC is now an established approach to many problems (Ellis *et al.*, 2014).

In summary, there may be a range of control objectives for renewable energy systems. Assuming, for the present study, that there is no obvious relationship between CapEx and control actions (though this comes under the gamut of control co-design, which has been examined for some renewable energy systems, e.g., (Pao *et al.*, 2023; Rosati and Ringwood, 2023)), the following individual objectives can be identified:

(a) Maximize power capture.
(b) Minimize the use of parasitic power consumption.
(c) Maximize the lifetime of the device.

For some renewable energy systems, the control actuator is typically the electrical generator itself (for example in the case of wave energy) while, in other domains, additional (energy consuming) actuation is required, for example with sluice gates in tidal barrages, or pitch/yaw control in wind turbines. Interestingly, in an effort to reduce pitch actuator power consumption, some turbine manufacturers have reduced the rated power of the actuators employed, leading to highly nonlinear saturating behavior (Leith and Leithead, 1997).

Most renewable energy systems are subject to physical constraints, which must be considered alongside the control objective, which could include constraints on displacements, velocities, and accelerations. A typical constrained control objective for a renewable energy system might look like:

$$\begin{gathered}\{y^{\mathrm{opt}}, f_{\mathrm{u}}^{\mathrm{opt}}\} = \underset{\{y, f_{\mathrm{u}}\}}{\operatorname{argmax}} E(y, f_{\mathrm{u}}),\\ \text{subject to :}\\ \text{Device dynamics } \mathcal{G}: \{\dot{x} = f(x, f_{\mathrm{e}}, f_{\mathrm{u}}), \quad y = Cx, \text{Constraints } \mathcal{S}: \{(y, f_{\mathrm{u}}) \in \mathcal{X} \times \mathcal{F}_{\mathrm{u}}, \quad \forall t \in \Omega,\end{gathered} \tag{4}$$

where y is typically some output variable (e.g. velocity, in the case of a wind turbine or wave device), and the map E represents the average converted energy of the system, i.e.,

$$E(y, f_{\mathrm{u}}) = \frac{1}{T_0} \int_{\Omega} y(\tau) f_{\mathrm{u}}(\tau) \mathrm{d}\tau. \tag{5}$$

y^{opt}, and $f_{\mathrm{u}}^{\mathrm{opt}}$, represents some optimal variable in the system (e.g. velocity), and the optimal energy-maximizing control solution, respectively. The sets $\mathcal{X}$ and $\mathcal{F}_{\mathrm{u}}$ represent the admissible values for output and input variables, i.e. constraints. Typically, the product $y(t)f_{\mathrm{u}}(t)$, representing instantaneous power, could be velocity × force, current × voltage, or flow × pressure.

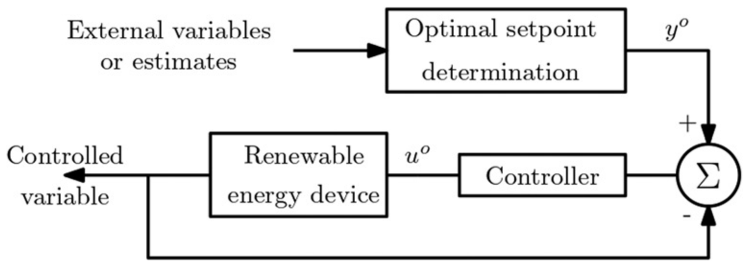

Fig. 17 Optimal setpoint determination, following by feedback tracking loop.

Minimization of multiple objectives (e.g. (a) to (c) above) can be achieved by extending the performance function in (5) to include other terms, but presents two difficulties:

- A relationship between the additional objective(s) and the control solution (f_u) must be found, and
- Suitable weighting factors, to balance the disparate quantities in the performance objective, must be found.

One alternative to the use of a composite performance function is multi-criteria optimization, (Aruldoss *et al.*, 2013) which essentially postpones any design decisions regarding the balance of objectives, but still requires each performance objective to be articulated in terms of the control signal.

Finally, especially given that many renewable energy devices are located in relatively remote/inaccessible locations, where maintenance opportunities may also be contingent on weather windows, it may be desired to have some level of fault tolerance built into the control. This has become a relatively established objective in the case of wind turbines, particularly relevant in the case of offshore devices (Shi and Patton, 2015).

Control Solution Domain

Within the physical confines of this chapter, it is impossible to give a comprehensive overview of all possible control solution strategies, across the range of renewable energy system types. Rather, an attempt will be made to look at applicable candidate solution concepts that match the problem specification in Section "Control Objectives". In addition to the control objectives articulated in Section"Control Objectives", there are a number of generic features of renewable energy systems that might help to define the control solution space:

i. Unlike more traditional control systems, disturbances are the active driving force, so need to be embraced, rather than rejected.
ii. In many cases, there is a need for prediction of disturbances, possibly with regard to use of MPC, also important in constraint handling,
iii. Since energy maximization is a typical objective, an obvious control solution candidate is extremum-seeking control, but there are issues to do with the stochastic nature of disturbances and satisfaction of hard constraints, and
iv. Many renewable energy systems are deployed as `farms', where interaction between individual devices can be constructive or destructive, often depending on control actions.

Typical control structure

A number of control problems in renewable energy systems are mainly characterized by classical regulatory, or setpoint following needs, for example in OTEC, salinity gradient, and solar heating. Other renewables require optimizing structures, to maximize energy conversion, such as solar PV, tidal, wind, and wave energy. However, some of these renewable types typically use an optimizing structure in tandem with a regulatory loop, namely wind, wave and tidal (flow and barrage). Such a control structure is illustrated in **Fig. 17**.

The upper branch in **Fig. 17** calculates an optimal setpoint for a key system variable, which is then followed by the lower regulatory loop. Key variables to be optimized (i.e. the y^o in **Fig. 17**) are shown in **Table 2**. The main challenge for the problem structure of **Fig. 17** is solving for the optimal setpoint, since no amount of good regulation, at the lower level, will compensate for an inaccurate setpoint. In some cases, especially given the bilinear nature of the control objective in (5), the optimization problem can be non-convex. Some solutions to this issue include the addition of regulatory terms to the performance function of (5), transcription of the problem effectively using an appropriate set of basis functions, (Faedo and Ringwood, 2024) or incorporation of a terminal cost into the performance function (Zhan *et al.*, 2024).

Disturbance/excitation estimation and forecasting

In many cases, key variables used in the control calculation are either difficult to measure, unmeasurable, or future values are needed, to allow optimal control calculations to be made, especially using predictive control methods. An interesting synergy exists where upwave, upwind, or upstream measurements may be made to provide advance knowledge of key inputs for wave, wind, and tidal systems respectively. In the case of renewable energy systems which rely on cyclical gravitational forces,i.e. tidal

Table 2 Key variables to be optimized for various renewable energy systems

Renewable system	*Wind*	*Tidal (flow)*	*Tidal (barrage)*	*Wave*
Key variable(s)	rotational speed	rotational speed	turbine flow sluice flow	velocity profile

stream and barrage systems, temporally accurate knowledge is known years in advance, though local weather conditions can have an additional minor influence. In the case of wave energy, even though the up-wave free surface can be measured, the key variable upon which the optimal control calculation is based, i.e. wave *excitation* force, (Ringwood *et al.*, 2014) is a variable derived from the free surface variations, and requires estimation (Peña-Sanchez *et al.*, 2019).

A variety of forecasting schemes for wind and wave systems have been developed, e.g., (Soman *et al.*, 2010; Pena-Sanchez *et al.*, 2018).

Typical control solutions

Extremum-seeking control Given the nature of the energy maximizing problem in (4), it would seem natural that an extremum-seeking control (ESC) approach would be appropriate. Indeed, this is a not uncommon approach for wind and solar systems, (Krstic *et al.*, 2014) particularly since the excitation is slowly varying. However, ESC is more challenging in the wave energy case, due to the stochastic nature of the disturbance and the need to allow a suitable integration time needed to capture a statistical measure of performance. As a result, only manipulation of `average' control settings can be managed with ESC, (Parrinello *et al.*, 2020) also characteristic of other learning control techniques (Anderlini *et al.*, 2018). An associated issue is the real-time satisfaction of hard system constraints with learning/ESC approaches (Pasta *et al.*, 2023).

Model predictive control Though model predictive control (MPC) was originally developed for the process industries, the flexibility of performance function specification allows a variety of performance functions to be articulated, including those related to energy, while economic MPC is also a current topical area (Zhan *et al.*, 2024). In many renewable energy applications, MPC is typically used to perform regulatory functions, with some notable exceptions. In wind energy, MPC is primarily used for regulation (speed control, control of power converter), but also for energy maximization (Cui *et al.*, 2018). In the wave energy case, a variety of MPC formulations have been proposed, (Faedo *et al.*, 2017) with the ability to effectively handle constraints an important feature. A typical (energy maximizing) MPC performance function is:

$$J(u) = \sum_{k=0}^{H_p} u_k x_k + q u_k^2 + r x_k^2 \tag{6}$$

where u is typically control force or voltage, while x is typically velocity or current, for example, with H_p the prediction horizon. The additional quadratic terms in u and x, while biasing the optimal energy capture solution, could have some benefit in providing `soft' constraints, but are usually used to convexify the performance function, though a terminal cost term can also be added for this purpose (Zhan *et al.*, 2024). MPC also sees applications in management of renewables on grid systems, (Qi *et al.*, 2012) but grid management is beyond the scope of this chapter.

Fault-tolerant control Given the often remote and inaccessible (e.g. offshore) nature of renewable energy parks/farms, and the potential unavailability of weather windows[1] for maintenance, there is significant interest in fault tolerant control (FTC), which may provide a level of system operation under fault conditions. In more mature renewables, such as wind energy, significant progress has been made on FTC, (Odgaard *et al.*, 2013) with FTC studies only beginning to emerge in less developed areas, such as tidal (Pham *et al.*, 2018) and wave (Zhang *et al.*, 2022).

Control of device farms

While, in a number of renewable energy modalities, each device effectively operates independently (e.g., solar PV panels), a number of renewable energy systems display significant interaction between devices. This interaction can be either destructive (e.g., tidal and wind[2]) or potentially constructive (e.g., wave (Bacelli *et al.*, 2013)). In arrays, since wave energy devices radiate waves by virtue of their own motion, this motion (which is a function of the control applied) can be used to reinforce the incoming waves to the mutual benefit of all the array elements. Up to 25% improvement in power capture is anticipated through the use of coordinated (global) array control, under real sea conditions (Bacelli *et al.*, 2013).

Application Study

Due to space constraints, it is not possible to cover a control application study for each renewable energy fom. Rather, a single illustrative example is chosen to show the nature of the control application, and the potential variety of control tools that can, or need to, be applied. The application chosen is from the wave energy area, which is one of the most challenging, given the

[1]We note that renewable devices are typically located in areas with significant wind/wave/tidal resources, which conflict with maintenance needs.
[2]We note that wake steering can be used in wind farms to minimize destructive interference (Howland *et al.*, 2019).

reciprocating and stochastic nature of the excitation and the difficulty of measurement of certain key variables. It also is the application area most familiar to this author!

A general approach to the control of wave energy systems is to use an (unknown input) estimator to estimate the wave excitation force, forecast future values of this excitation, and then use some form of optimizing real-time control (Korde and Ringwood, 2016). However, some novel wave energy control philosophies have been proposed, including one which treats the panchromatic excitation as an instantaneous monochromatic signal, the frequency and amplitude of which is estimated using an extended Kalman filter (EKF), resulting in relatively simple control calculations, and constraint handling (Fusco and Ringwood, 2012).

System Model

A schematic of the wave energy system to be controlled is shown in **Fig. 18**, while the system is defined (in the frequency domain) by Eq. (7), following Newton's second law, and assuming linear hydrodynamics:

$$j\omega MV(\omega) + Z_r(\omega)V(\omega) + \frac{K_s}{j\omega} = F_{ex}(\omega) + F_u(\omega), \tag{7}$$

with $Z_r(\omega) = H_r(\omega) + j\omega M_\infty$. The model in (7) can be expressed in the compact form:

$$V(\omega) = \frac{1}{Z_i(\omega)}[F_{ex}(\omega) + F_u(\omega)], \tag{8}$$

where the intrinsic impedance, $Z_i(\omega)$, is defined as:

$$Z_i(\omega) = B(\omega) + j\omega\left[M + M_a(\omega) + M_\infty - \frac{K_s}{\omega^2}\right]. \tag{9}$$

Note that $B(\omega)$, $M_a(\omega)$, and M_∞ are typically determined from panelised boundary-element hydrodynamic codes, such as Nemoh, (Babarit and Delhommeau, 2015) which return non-parametric frequency-domain data. The excitation force is the effect of the incident wave on the floating system:

$$F_{ex}(\omega) = H_{ex}(\omega)(\Xi)(\omega), \tag{10}$$

where $(\Xi)(\omega)$ is the Fourier transform of the incident wave elevation, $\eta(t)$. The example WEC system considered in this study consists of a heaving cylinder with radius $R = 3$ m, height $H = 5$ m, draught $h = 4$ m, mass $M = 3.2 \times 10^5$ Kg. The radiation and excitation transfer functions, $H_r(\omega)$ and $H_{ex}(\omega)$, are shown in **Fig. 19**.

For the geometry specified in **Fig. 19**, a 4^{th}-order parametric approximation for the radiation term is calculated using frequency-domain identification, following the approach in (Faedo *et al.*, 2018). The result, shown in **Fig. 19**(a), gives an accurate approximation of the radiation response of the system. An overall 6^{th} order force-velocity system model is therefore obtained as:

$$\frac{1}{Z_i(s)} = \frac{1.8 \times 10^{-6} \cdot s(s^2 + 1.1s + 0.4)(s^2 + 1.6s + 1.8)}{(s^2 + 1.2s + 0.4)(s^2 + 1.4s + 1.6)(s^2 + 0.1s + 1.5)}. \tag{11}$$

Controller Development

From Falnes and Kurniawan (2020) maximum energy transfer from the waves to the system PTO is obtained when:

$$F_u(\omega) = -Z_i^*(\omega)V(\omega), \tag{12}$$

which is equivalent to the maximum power transfer theorem for AC circuits. (12) can be recast as gain and (zero) phase

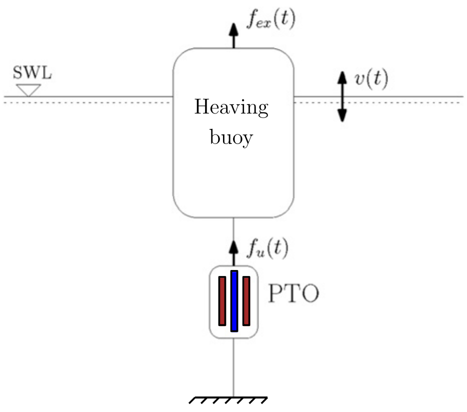

Fig. 18 One-degree of freedom (heave) floating system for wave energy conversion. The PTO typically contains a linear generator. SWL corresponds to the still water level, f_{ex} the wave excitation force, $v(t)$ the device velocity, while $f_u(t)$ is the applied control (load) force.

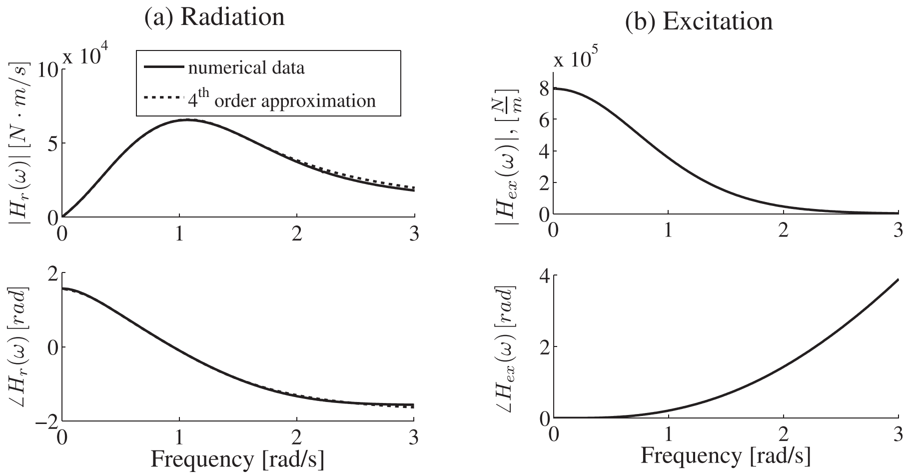

Fig. 19 Radiation and excitation frequency responses for a floating cylinder with radius $R = 3$ m, height $H = 5$ m, draught $h = 4$ m, mass $M = 3.2 \times 10^5$ Kg. Note that a 4th order parametric approximation is calculated for $H_r(\omega)$.

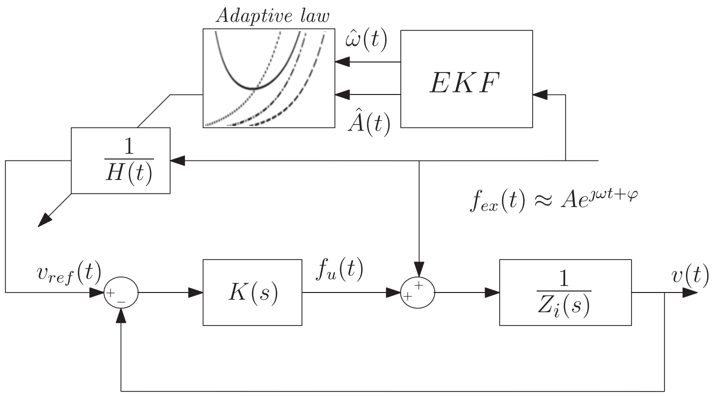

Fig. 20 Control architecture for the 'Simple and Effective' wave energy controller. The upper branch determines the optimal velocity reference, in the spirit of Fig. 17, while the lower loop ensures tracking of $v_{ref}(t)$.

conditions:

$$V(\omega) = \frac{1}{Z_i(\omega) + Z_i^*(\omega)} F_{ex}(\omega) = \frac{1}{2B(\omega)} F_{ex}(\omega), \tag{13}$$

where $B(\omega)$ is a real and even function. Since the relation in (13) is a frequency-dependent gain, an assumption is made that the excitation, $f_{ex}(t)$, is a narrow-band harmonic process, defined by time-varying amplitude $A(t)$, frequency $\omega(t)$, and phase $\varphi(t)$:

$$f_{ex}(t) = A(t)\cos(\omega(t)t + \varphi(t)), \tag{14}$$

so the reference velocity can be generated from the following adaptive law:

$$v_{ref}(t) = \frac{1}{H(t)} f_{ex}(t), \quad \frac{1}{H(t)} = \frac{1}{2B(\hat{\omega})} \tag{15}$$

where $H(t)$ is calculated from the $1/2B(\omega)$ curve, based on a real-time estimate of the peak frequency of the wave excitation force $\hat{\omega}$, provided from an extended Kalman filter (EKF) The EKF also supplies an estimate $\hat{A}$ in (14) at $\hat{\omega}$.

Constraint Handling

As a consequence of the proportional reference-generation law in (15), the complex amplitude of the velocity, $\hat{V}$, and position, $\hat{X}$, can be expressed as:

$$\hat{V} = \frac{A}{H} e^{j\varphi}, \quad \hat{X} = \frac{\hat{V}}{j\omega} = \frac{A}{j\omega H} e^{j\varphi}, \tag{16}$$

and, if the vertical excursion of the WEC is limited to $\pm X_{lim}$ m from equilibrium, the position constraint can be written as an equivalent velocity constraint:

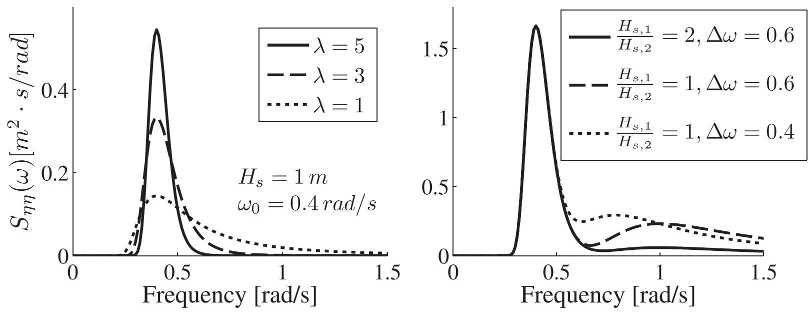

Fig. 21 Spectral shapes, derived from the Ochi model in (19), utilized for wave simulation.

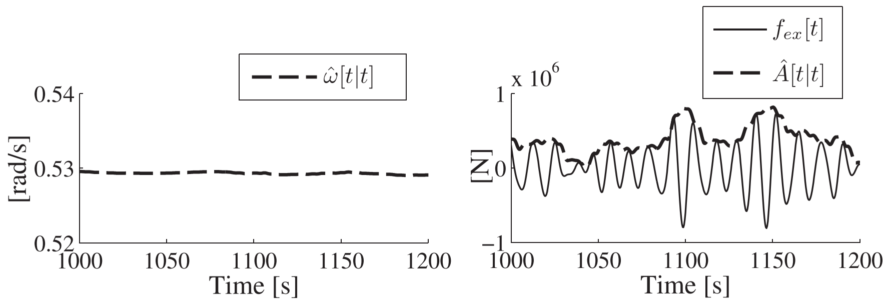

Fig. 22 Real-time estimation of amplitude and frequency of a stochastic excitation-force signal, generated from a power spectral distribution centered around 5.3 rad/s.

$$\hat{X} = \frac{\hat{V}}{j\omega} \le X_{lim} \quad \Leftrightarrow \quad |\hat{V}| \le \omega X_{lim}. \tag{17}$$

An upper bound for the variable gain, $1/H(t)$, involving the amplitude and frequency of the excitation, can then be derived from Eq. (16) as:

$$\frac{1}{H} \le \frac{\omega X_{lim}}{A}. \tag{18}$$

The overall control system architecture is shown in **Fig. 20**.

Note that a variety of controllers can be utilized to perform velocity tracking, and are not detailed here. Two possibilities, employed with the controller architecture in **Fig. 20**, are internal model control (IMC) (Fusco and Ringwood, 2012) and robust control, based on passivity (Fusco and Ringwood, 2014). Results based on an IMC controller are detailed in Section "Sample Results".

Sample Results

Random waves are generated from single- and double-peaked standard wave spectral distributions. The 3- and 6-parameters Ochi spectral distributions (Ochi, 1998) are utilized, which give the possibility of independently specifying the modal frequency, ω_0, the significant wave height, H_s, and the sharpness, λ:

$$S_{\eta\eta}(\omega) = \sum_{j=1,2} \frac{\left(\frac{4\lambda_j+1}{4}\omega_{0,j}^4\right)^{\lambda_j}}{\Gamma(\lambda_j)} \cdot \frac{H_{s,j}^2}{\omega^{4\lambda_j+1}} e^{-\left(\frac{4\lambda_j+1}{4}\right)\left(\frac{\omega_{0,j}}{\omega}\right)^4} \tag{19}$$

where $j = 1, 2$ are the components of the spectrum (only $j = 1$ for the single-peak case) and $\Gamma(\cdot)$ is a Gamma function.

Fig. 21 shows some examples of the wave spectral distributions. The double-peak spectra are parameterized with the ratio $H_{s,1}/H_{s,2}$, that is the relative energy of the two peaks, with a spacing between the peaks of $\Delta\omega = \omega_{0,2} - \omega_{0,1}$. A variety of single-peak spectra has been chosen with ω_0 ranging from 0.3 to 1.2 rad/s, λ from 0.5 to 5 (wide- to narrow-banded spectrum) and $H_s = 1$ or $H_s = 3$ m. For the double-peaked spectra the ratio $H_{s,1}/H_{s,2}$ ranges from 4 to 0.5; the frequency spacing, $\Delta\omega$, ranges from 0.2 to 0.9 rad/s.

Real-time instantaneous estimates of amplitude and frequency for the stochastic excitation-force signal are shown in **Fig. 22**.

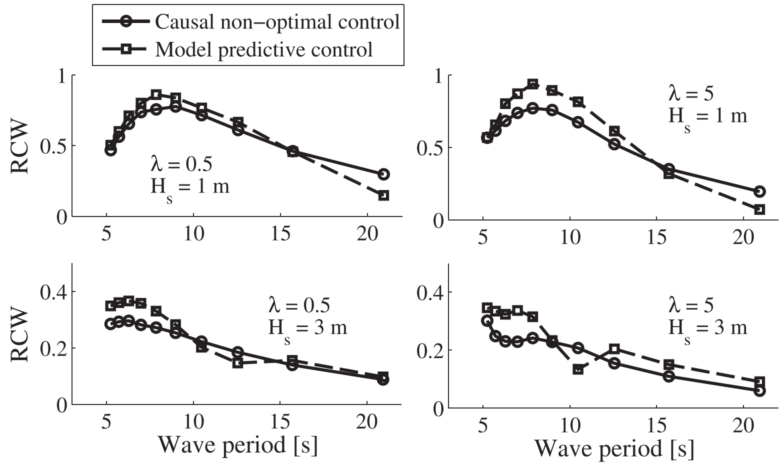

Fig. 23 Performance, in terms of relative capture width (RCW).

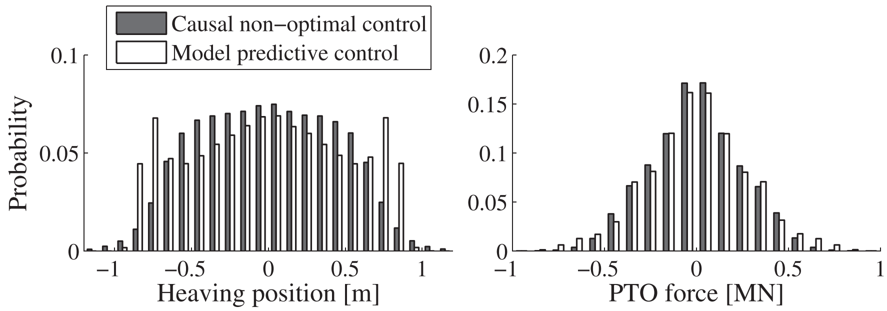

Fig. 24 Distribution of heave excursion and PTO force.

Overall control performance is measured in terms of relative capture width (RCW):

$$RCW = \frac{\overline{P}_u}{2RP_w}, \tag{20}$$

which is the ratio between average absorbed power, $\overline{P}_u$, and average wave power, P_w, over a front as wide as the cylinder ($2R$). Note that deep water is assumed, so that the wave power, per meter of wave front, is calculated from the wave spectral distribution, $S_{\eta\eta}(\omega)$, as (Falnes and Kurniawan, 2020):

$$P_w = \frac{\rho g^2}{2}\int_0^{\infty}\frac{S_{\eta\eta}(\omega)}{\omega}d\omega \qquad \left[\frac{W}{m}\right], \tag{21}$$

where ρ is the water density and g is the acceleration due to gravity.

As a reference, MPC is utilized for comparison, following the approach proposed by Hals *et al.* (2011). The MPC prediction horizon (H_p in (6)) is set to 30 steps ($\approx$11.77 s), which is about double the resonance period of the floating cylinder ($\approx 5.2s$). For a fair comparison, f_{ex} predictions are not assumed to be ideal and a forecasting algorithm, based on an AR model, is implemented (Pena-Sanchez *et al.*, 2018). **Fig. 23** shows the *RCW* obtained from the two controllers, in wide- ($\lambda = 0.5$) and narrow-banded ($\lambda = 5$) sea , for different peak periods, $2\pi/\omega_0$. Two significant wave heights, $H_s = 1$ and $H_s = 3$ m, are also utilized.

The `Simple and Effective' sub-optimal controller performs quite closely to MPC for both short and long waves, but is less efficient around the resonant peak, possibly due to the approximate constraint handling, which is separately illustrated in **Fig. 24**.

Conclusions

This chapter attempts to provide some level of detail in relation to the type of control problems, and some control solution concepts, that arise in renewable energy systems. Due to the wide variety of renewable energy systems, it is not possible to provide a comprehensive treatment of all renewables, but hopefully a flavor of typical problems, and their contrast with some more traditional control problem specifications, has been given. A number of associated control problems that arise with renewable energy systems, but are not treated in this chapter, include the important areas of the incorporation of intermittent renewable energy systems into electricity grids, (Al-Shetwi *et al.*, 2020) and the incorporation of various energy storage modalities, on different time scales (Damiano *et al.*, 2013).

Taking an even broader view, the scale of the challenge in satisfying energy demand with zero-carbon renewable energy is dependent on the scale of the demand itself, which can also be mitigated using control methods (Strbac, 2008).

Acknowledgments

The author is grateful for the support of MaREI, the SFI Research Centre for Energy, Climate and Marine, Ireland, under Grant No. 12/RC/2302_P2, and is grateful for the inspiration provided by many collaborators, colleagues, postdocs, and PhD students.

References

Alam, M.S., Al-Ismail, F.S., Salem, A., Abido, M.A., 2020. High-level penetration of renewable energy sources into grid utility: Challenges and solutions. IEEE Access 8, 190277–190299.
Allouhi, A., Rehman, S., Buker, M.S., Said, Z., 2022. Up-to-date literature review on solar pv systems: Technology progress, market status and r&d. Journal of Cleaner Production 362, 132339.
Al-Shahri, O.A., Ismail, F.B., Hannan, M., *et al.*, 2021. Solar photovoltaic energy optimization methods, challenges and issues: A comprehensive review. Journal of Cleaner Production 284, 125465.
Al-Shetwi, A.Q., Hannan, M., Jern, K.P., Mansur, M., Mahlia, T.M.I., 2020. Grid-connected renewable energy sources: Review of the recent integration requirements and control methods. Journal of Cleaner Production 253, 119831.
Anderlini, E., Forehand, D., Bannon, E., Xiao, Q., Abusara, M., 2018. Reactive control of a two-body point absorber using reinforcement learning. Ocean Engineering 148, 650–658.
Angeloudis, A., Kramer, S.C., Avdis, A., Piggott, M.D., 2018. Optimising tidal range power plant operation. Applied Energy 212, 680–690.
Aruldoss, M., Lakshmi, T.M., Venkatesan, V.P., 2013. A survey on multi criteria decision making methods and its applications. American Journal of Information Systems 1 (1), 31–43.
Awasthi, A., Shukla, A.K., MM, S.R., *et al.*, 2020. Review on sun tracking technology in solar pv system. Energy Reports 6, 392–405.
Babarit, A., Delhommeau, G., 2015. Theoretical and numerical aspects of the open source bem solver nemoh. In: Proceedings of the 11th European Wave and Tidal Energy Conference (EWTEC), Nantes .
Bacelli, G., Balitsky, P., Ringwood, J.V., 2013. Coordinated control of arrays of wave energy devices-benefits over independent control. IEEE Transactions on Sustainable Energy 4 (4), 1091–1099.
Bacelli, G., Gilloteaux, J.C., Ringwood, J., 2009. A predictive controller for a heaving buoy producing potable water. In: Proceedings of the 2009 European Control Conf. (ECC), Budapest , 3755–3760 .
Bhattacharya, S., Nikitas, G., Jalbi, S., 2018. On the use of scaled model tests for analysis and design of offshore wind turbines. Geotechnics for Natural and Engineered Sustainable Technologies. Springer. pp. 107–129.
Camacho E.F., Berenguel M., 2012. Control of solar energy systems . IFAC Proceedings Volumes 45 (15): 848–855.
Chen, W.H., 2024. Goal-oriented control systems (GOCS): From HOW to WHAT. IEEE/CAA Journal of Automatica Sinica 11 (4), 816–819.
Cohen, R., 2009. 05 , An overview of ocean thermal energy technology, potential market applications, and technical challenges. In: Proceedings of the OTC Offshore Technology Conference .
Cui, J., Liu, S., Liu, J., Liu, X., 2018. A comparative study of MPC and economic MPC of wind energy conversion systems. Energies 11 (11), 3127.
Damiano, A., Gatto, G., Marongiu, I., Porru, M., Serpi, A., 2013. Real-time control strategy of energy storage systems for renewable energy sources exploitation. IEEE Transactions on Sustainable Energy 5 (2), 567–576.
Ellis, M., Durand, H., Christofides, P.D., 2014. A tutorial review of economic model predictive control methods. Journal of Process Control 24 (8), 1156–1178.
Faedo, N., Ringwood, J.V., 2024. A control framework for ocean wave energy conversion systems: The potential of moments. Annual Review of Control, Robotics, and Autonomous Systems 7.
Faedo, N., Olaya, S., Ringwood, J.V., 2017. Optimal control, MPC and MPC-like algorithms for wave energy systems: An overview. IFAC Journal of Systems and Control 1, 37–56.
Faedo, N., Peña-Sanchez, Y., Ringwood, J.V., 2018. Finite-order hydrodynamic model determination for wave energy applications using moment-matching. Ocean Engineering 163, 251–263.
Falnes, J., Kurniawan, A., 2020. Ocean Waves and Oscillating Systems: Linear Interactions Including Wave-Energy Extraction, second ed. Cambridge University Press.
Fenu, B., Attanasio, V., Casalone, P., *et al.*, 2020. Analysis of a gyroscopic-stabilized floating offshore hybrid wind-wave platform. Journal of Marine Science and Engineering 8 (6), 439.
Fontanella, A., Belloli, M., 2021. Model-inversion feedforward control for wave load reduction in floating wind turbines. In: Proceedings of the International Conference on Offshore Mechanics and Arctic Eng. (OMAE) , 61923, pp. 1–9 .
Frederik, J.A., Doekemeijer, B.M., Mulders, S.P., van Wingerden, J.W., 2020. The helix approach: Using dynamic individual pitch control to enhance wake mixing in wind farms. Wind Energy 23 (8), 1739–1751.
Fuentes-Morales, R.F., Diaz-Ponce, A., Peña-Cruz, M.I., *et al.*, 2020. Control algorithms applied to active solar tracking systems: A review. Solar Energy 212, 203–219.
Fusco, F., Ringwood, J.V., 2012. A simple and effective real-time controller for wave energy converters. IEEE Trans. on Sustainable Energy 4 (1), 21–30.
Fusco, F., Ringwood, J.V., 2014. Hierarchical robust control of oscillating wave energy converters with uncertain dynamics. IEEE Transactions on Sustainable Energy 5 (3), 958–966.
Fusco, F., Nolan, G., Ringwood, J.V., 2010. Variability reduction through optimal combination of wind/wave resources-an Irish case study. Energy 35 (1), 314–325.
Gonzales, R.R., Abdel-Wahab, A., Adham, S., *et al.*, 2021. Salinity gradient energy generation by pressure retarded osmosis: A review. Desalination 500, 114841.
Hals, J., Falnes, J., Moan, T., 2011. Constrained optimal control of a heaving buoy wave-energy converter. Journal of Offshore Mechanics and Arctic Engineering 133, 011401-1–011401-15.
Hand, B., Kelly, G., Cashman, A., 2021. Aerodynamic design and performance parameters of a lift-type vertical axis wind turbine: A comprehensive review. Renewable and Sustainable Energy Reviews 139, 110699.
Hau, E., Renouard, H., 2006. Wind Turbines: Fundamentals, Technologies, Application, Economics. Springer.

He, X., He, W., Liu, Y., *et al.*, 2018. Robust adaptive control of an offshore ocean thermal energy conversion system. IEEE Transactions on Systems, Man, and Cybernetics 50 (12), 5285–5295.
Herrera, J., Sierra, S., Ibeas, A., 2021. Ocean thermal energy conversion and other uses of deep sea water: A review. Journal of Marine Science and Engineering 9 (4), 356.
Howland, M.F., Lele, S.K., Dabiri, J.O., 2019. Wind farm power optimization through wake steering . In: Proceedings of the National Academy of Sciences 116 (29), pp. 14495-14500 .
Ibrahim, B.S., Shareef, S.J.M., Ameen, H.F., 2021. Performance analysis of photovoltaic panels under the effect of electrical and environmental parameters in Erbil city. UKH Journal of Science and Engineering 5 (1), 101–110.
International Energy Agency, 2023. Renewable energy progress tracker . https://www.iea.org/data-and-statistics/data-tools/renewable-energy-progress-tracker . (accessed: 03.12.24).
Jelavić, M., Petrović, V., Perić, N., 2010. Estimation based individual pitch control of wind turbine. Automatika 51 (2), 181–192.
Johnson, K.E., Pao, L.Y., Balas, M.J., Fingersh, L.J., 2006. Control of variable-speed wind turbines: Standard and adaptive techniques for maximizing energy capture. IEEE Control Systems Magazine 26 (3), 70–81.
Jurasz, J., Canales, F., Kies, A., Guezgouz, M., Beluco, A., 2020. A review on the complementarity of renewable energy sources: Concept, metrics, application and future research directions. Solar Energy 195, 703–724.
Kempener, R., Neumann, F., 2014. Salinity gradient energy technology brief . , International Renewable Energy Agency (IRENA).
Khare, V., Khare, C., Nema, S., Baredar, P., 2018. Tidal Energy Systems: Design. Optimization and Control. Elsevier.
Koca, K., Kortenhaus, A., Oumeraci, H., *et al.*, 2013. Recent advances in the development of wave energy converters. In: Proceedings of the 9th European Wave and Tidal Energy Conference (EWTEC), Aalborg .
Korde, U.A., Ringwood, J., 2016. Hydrodynamic Control of Wave Energy Devices. Cambridge University Press.
Krstic, M. , Ghaffari, A., Seshagiri, S., 2014. Extremum seeking for wind and solar energy applications. In: Proceedings of the 11th World Congress on Intelligent Control and Automation. pp. 6184–6193.
Langer, J., Quist, J., Blok, K., 2020. Recent progress in the economics of ocean thermal energy conversion: Critical review and research agenda. Renewable and Sustainable Energy Reviews 130, 109960.
Leith, D.J., Leithead, W., 1997. Implementation of wind turbine controllers. International Journal of Control 66 (3), 349–380.
Morlais, 2022. What do tidal energy device look like? https://www.morlaisenergy.com/tidal-energy/ . [Online; accessed 21-01-2022] .
Narayana, M. , Putrus, G. , Jovanovic, M., Leung, P.S., 2009. Predictive control of wind turbines by considering wind speed forecasting techniques. In: Proceedings of the 2009 44th International Universities Power Engineering Conference (UPEC). pp. 1–4.
Ochi, M., 1998. Ocean waves: The stochastic approach. Oceanographic Literature Review 6 (45), 904.
Odgaard, P.F., Stoustrup, J., Kinnaert, M., 2013. Fault-tolerant control of wind turbines: A benchmark model. IEEE Trans. on Control Systems Technology 21 (4), 1168–1182.
Orbital Marine Power, 2024. Orbital marine power. https://www.orbitalmarine.com/technology/, year = 2024, note = (accessed: 2024-13-03.24).
Ourahou, M., Ayrir, W., Hassouni, B.E., Haddi, A., 2020. Review on smart grid control and reliability in presence of renewable energies: Challenges and prospects. Mathematics and Computers in Simulation 167, 19–31.
Pao, L.Y., Pusch, M., Zalkind, D.S., 2023. Control co-design of wind turbines. Annual Review of Control, Robotics, and Autonomous Systems. 7.
Parrinello, L., Dafnakis, P., Pasta, E., *et al.*, 2020. An adaptive and energy-maximizing control optimization of wave energy converters using an extremum-seeking approach. Physics of Fluids 32 (11),
Pasta, E., Faedo, N., Mattiazzo, G., Ringwood, J.V., 2023. Towards data-driven and data-based control of wave energy systems: Classification, overview, and critical assessment. Renewable and Sustainable Energy Reviews 188, 113877.
Pattle, R., 1954. Production of electric power by mixing fresh and salt water in the hydroelectric pile. Nature 174 (4431), 660-660.
Pena-Sanchez, Y., Mérigaud, A., Ringwood, J.V., 2018. Short-term forecasting of sea surface elevation for wave energy applications: The autoregressive model revisited. IEEE Journal of Oceanic Engineering 45 (2), 462–471.
Peña-Sanchez, Y., Windt, C., Davidson, J., Ringwood, J.V., 2019. A critical comparison of excitation force estimators for wave-energy devices. IEEE Transactions on Control Systems Technology 28 (6), 2263–2275.
Pham, H.T., Bourgeot, J.M., Benbouzid, M., 2018. Fault-tolerant finite control set-model predictive control for marine current turbine applications. IET Renewable Power Generation 12 (4), 415–421.
Qazi, A., Hussain, F., Rahim, N.A., *et al.*, 2019. Towards sustainable energy: a systematic review of renewable energy sources, technologies, and public opinions. IEEE Access 7, 63837–63851.
Qi, W., Liu, J., Christofides, P.D., 2012. Distributed supervisory predictive control of distributed wind and solar energy systems. IEEE Transactions on Control Systems Technology 21 (2), 504–512.
Ringwood, J.V., Faedo, N., 2022. Tidal barrage operational optimisation using wave energy control techniques. IFAC-PapersOnLine 55 (31), 148–153.
Ringwood, J.V., Bacelli, G., Fusco, F., 2014. Energy-maximizing control of wave-energy converters: The development of control system technology to optimize their operation. IEEE Control Systems Magazine 34 (5), 30–55.
Rosati, M., Ringwood, J.V., 2023. Control co-design of power take-off and bypass valve for OWC-based wave energy conversion systems. Renewable Energy 219, 119523.
Ryrie, S., 1995. An optimal control model of tidal power generation. Applied Mathematical Modelling 19 ((2), 123–126.
Sarmiento, J., Iturrioz, A., Ayllón, V., Guanche, R., Losada, I., 2019. Experimental modelling of a multi-use floating platform for wave and wind energy harvesting. Ocean Engineering 173, 761–773.
Selvam, K., Kanev, S., van Wingerden, J.W., van Engelen, T., Verhaegen, M., 2009. Feedback–feedforward individual pitch control for wind turbine load reduction. International Journal of Robust and Nonlinear Control 19 (1), 72–91.
Sharaf, M., Yousef, M.S., Huzayyin, A.S., 2022. Review of cooling techniques used to enhance the efficiency of photovoltaic power systems. Environmental Science and Pollution Research 29 (18), 26131–26159.
Shen, Y., Nyman, P.O., 2021. Optimal operation of tidal plants based on nonlinear model predictive control strategy. IOP Conference Series: Earth and Environmental Science 687 (1), 012101.
Shi, F., Patton, R., 2015. An active fault tolerant control approach to an offshore wind turbine model. Renewable Energy 75, 788–798.
Sinsel, S.R., Riemke, R.L., Hoffmann, V.H., 2020. Challenges and solution technologies for the integration of variable renewable energy sources-a review. Renewable Energy 145, 2271–2285.
Skaare, B. , Hanson, T.D., Nielsen, F.G.,2007. Importance of control strategies on fatigue life of floating wind turbines. In: Proceedings of the International Conference on Offshore Mechanics and Arctic Eng. (OMAE) , 42711. pp. 493–500.
Soman, S.S., Zareipour, H., Malik, O., Mandal, P., 2010. A review of wind power and wind speed forecasting methods with different time horizons. In: Proceedings of the North American Power Symposium. pp. 1–8.
Strbac, G., 2008. Demand side management: Benefits and challenges. Energy Policy 36 (12), 4419–4426.
Tan, K.M., Babu, T.S., Ramachandaramurthy, V.K., *et al.*, 2021. Empowering smart grid: A comprehensive review of energy storage technology and application with renewable energy integration. Journal of Energy Storage 39, 102591.
Tristán, C., Fallanza, M., Ibáñez, R., Ortiz, I., 2020. Recovery of salinity gradient energy in desalination plants by reverse electrodialysis. Desalination 496, 114699.

Tufa, R.A., Pawlowski, S., Veerman, J., *et al.*, 2018. Progress and prospects in reverse electrodialysis for salinity gradient energy conversion and storage. Applied Energy 225, 290–331.

Walker, S., Thies, P., 2021. A review of component and system reliability in tidal turbine deployments. Renewable and Sustainable Energy Reviews 151, 111495.

Windt, C., Faedo, N., Penalba, M., Dias, F., Ringwood, J.V., 2021. Reactive control of wave energy devices-the modelling paradox. Applied Ocean Research 109, 102574.

Zhan, S., Chen, Y., Ringwood, J.V., 2024. Terminal weight and constraint design for wave energy converter economic model predictive control problems. In: Proceedings of the International Journal of Robust and Nonlinear Control (early access) .

Zhang, Y., Zeng, T., Gao, Z., 2022. Fault diagnosis and fault-tolerant control of energy maximization for wave energy converters. IEEE Transactions on Sustainable Energy 13 (3), 1771–1778.